University of New Hampshire
University of New Hampshire Scholars' Repository

Physics Scholarship

Physics

3-1-1998

AMPTE/CCE-SCATHA simultaneous observations of substorm-associated magnetic fluctuations

S. Ohtani

K. Takahashi

T. Higuchi

A. T. Y. Lui

Harlan E. Spence
Boston University, harlan.spence@unh.edu

See next page for additional authors

Follow this and additional works at: https://scholars.unh.edu/physics_facpub

Part of the Physics Commons

Recommended Citation

Authors

S. Ohtani, K. Takahashi, T. Higuchi, A. T. Y. Lui, Harlan E. Spence, and J. F. Fennell

AMPTE/CCE–SCATHA simultaneous observations of substorm-associated magnetic fluctuations

S. Ohtani,[1] K. Takahashi,[2] T. Higuchi,[3] A. T. Y. Lui,[1] H. E. Spence,[4] and J. F. Fennell[5]

Abstract. This study examines substorm-associated magnetic field fluctuations observed by the AMPTE/CCE and SCATHA satellites in the near-Earth tail. Three tail reconfiguration events are selected, one event on August 28, 1986, and two consecutive events on August 30, 1986. The fractal analysis was applied to magnetic field measurements of each satellite. The result indicates that (1) the amplitude of the fluctuation of the north–south magnetic component is larger, though not overwhelmingly, than the amplitudes of the other two components and (2) the magnetic fluctuations do have a characteristic timescale, which is several times the proton gyroperiod. In the examined events the satellite separation was less than 10 times the proton gyroradius. Nevertheless, the comparison between the AMPTE/CCE and SCATHA observations indicates that (3) there was a noticeable time delay between the onsets of the magnetic fluctuations at the two satellite positions, which is too long to ascribe to the propagation of a fast magnetosonic wave, and (4) the coherence of the magnetic fluctuations was low in the August 28, 1986, event and the fluctuations had different characteristic timescales in the first event of August 30, 1986, whereas some similarities can be found for the second event of August 30, 1986. Result 1 indicates that perturbation electric currents associated with the magnetic fluctuations tend to flow parallel to the tail current sheet and are presumably related to the reduction of the tail current intensity. Results 2 and 3 suggest that the excitation of the magnetic fluctuations and therefore the trigger of the tail current disruption is a kinetic process in which ions play an important role. It is inferred from results 3 and 4 that the characteristic spatial scale of the associated instability is of the order of the proton gyroradius or even shorter, and therefore the tail current disruption is described as a system of chaotic filamentary electric currents. However, result 4 suggests that the nature of the tail current disruption can vary from event to event.

1. Introduction

We recently reached a new conjecture about the substorm trigger, which is often referred to as the Kiruna conjecture [*Kennel*, 1992]. The conjecture suggests that the near-Earth magnetotail is an important region for the substorm trigger. Examples of supporting evidence for this include (1) turbulent magnetic field variations in the near-Earth region ($r \approx 8\ R_E$) that start simultaneously with a ground substorm onset [*Takahashi et al.*, 1987; *Lui et al.*, 1988, 1992; *Lopez et al.*, 1989]; (2) time delay of dipolarization signatures observed by multisatellites in the synchronous region [*Lopez et al.*, 1990; *Lopez and Lui*, 1990; *Ohtani et al.*, 1991, 1993]; (3) tailward expansion of tail current disruption observed at $r < 15\ R_E$ [*Jacquey et al.*, 1991, 1993; *Ohtani et al.*, 1992a]; (4) modeling

of the buildup of the tail current intensity in the near-Earth tail based on satellite magnetic field measurements [*Kaufmann*, 1987; *Pulkkinen et al.*, 1991]; (5) mapping of initial brightening aurorae toward the equatorial plane in the near-Earth tail [*Elphinstone et al.*, 1991; *Samson et al.*, 1992]; and (6) the formation of a substorm-associated field-aligned current system well equatorward of the open/closed boundary [*Lopez et al.*, 1991].

To understand substorm trigger mechanisms, it should be reasonable to examine substorm signatures observed in the near-Earth region. The characteristic timescale and spatial scale of magnetic fluctuations associated with tail current disruption, especially, should place important constraints on substorm trigger models. *Lui et al.* [1992] reported 15 substorm events in which turbulent magnetic fields were observed by the AMPTE/CCE satellite near the equator. Among these events the event that occurred on August 28 (day 240), 1986, provides a unique opportunity because the satellite was in a tail current disruption region at a substorm onset and remained in the region for as long as 3 min. The event was originally reported by *Takahashi et al.* [1987] and was examined later by *Lui et al.* [1992] and *Burkhart et al.* [1993] from different viewpoints.

In our previous study [*Ohtani et al.*, 1995; hereinafter referred to as paper 1] we also reexamined this event, as well as the other AMPTE/CCE tail current disruption events, by applying the fractal analysis [*Higuchi*, 1988, 1990] to the observed magnetic fluctuations. We found that (1) the magnetic fluctua-

---

[1]Applied Physics Laboratory, The Johns Hopkins University, Laurel, Maryland.

[2]Solar-Terrestrial Environment Laboratory, Nagoya University, Toyokawa, Japan.

[3]Institute of Statistical Mathematics, Tokyo, Japan.

[4]Center for Space Physics, Boston University, Boston, Massachusetts.

[5]Aerospace Corporation, Los Angeles, California

tions have a characteristic timescale, which is several times the proton gyroperiod, and (2) the magnitude of the H (north–south) component fluctuations is larger than that of the other components by about 30%, suggesting that associated electric currents flow in various directions but flow preferentially parallel to the neutral sheet. From these results we inferred that these fluctuations are related to the trigger of the tail current disruption and that ions play an important role in their excitation.

In this study we extend our previous analysis of the August 28, 1986, event by examining simultaneous magnetic field measurements from the SCATHA satellite, which we found stayed at or near the neutral sheet separated from AMPTE/CCE by 0.5 R_E in the radial direction and 0.5 hour in magnetic local time (MLT). In addition, we examine an AMPTE/CCE and SCATHA conjunction event that took place on August 30 (day 242), 1986. In this event the separation between AMPTE/CCE and SCATHA was even smaller, only 0.4 R_E. These fortunate opportunities allow us to address the spatial as well as the temporal characteristics of the magnetic fluctuations. In section 2 we describe these two substorm events and the results of the fractal analysis. In section 3 we discuss the timescale and spatial scale of the magnetic fluctuations and address constraints that the present study can place on substorm trigger models. Section 4 is a summary.

2. Observations

2.1. August 28 (Day 240), 1986, Event

2.1.1. Overall features. Figure 1 shows the locations of the AMPTE/CCE and SCATHA satellites projected onto the
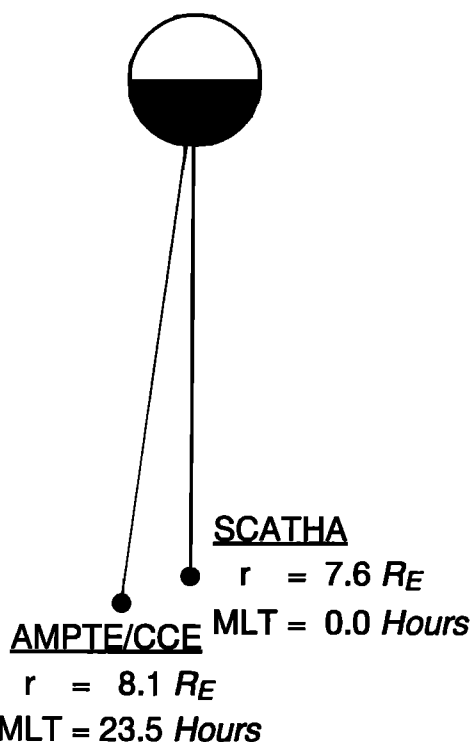

Figure 1. Locations of the AMPTE/CCE and SCATHA satellites for the August 28 (day 240), 1986, event projected onto the equatorial plane.

equatorial plane. AMPTE/CCE was at r (radial distance) = 8.1 R_E and MLT = 23.5, whereas SCATHA was at r = 7.6 R_E and MLT = 0.0. The magnetic latitudes of AMPTE/CCE and SCATHA were $-2.3°$ and $-2.9°$, respectively. The satellite separation was 0.5 R_E in radial distance and 0.5 hour in local time.

Figure 2 plots the Kakioka Pi2 (differentiated north–south, H, magnetic component; invariant latitude: 25.6°; MLT: 21.1) data and three magnetic field components and total field strength observed by AMPTE/CCE and SCATHA during the 10-min interval of 1150 to 1200 UT (see *Takahashi et al.* [1987, Figure 1] for longer time span plots of the Kakioka and AMPTE/CCE data). Figure 3 is a close-up of the subinterval of 1152:15 to 1156:45 UT for the satellite data. See *Potemra et al.* [1985] and *Fennell* [1982] for the details of the magnetometers on board AMPTE/CCE and SCATHA, respectively. The time resolution of the data used in Figures 2 and 3 is 0.25 s for both satellites. The magnetometer data are presented in the *VDH* coordinate system. In this coordinate system, H is antiparallel to the Earth's dipole axis, V points radially outward and is parallel to the magnetic equator, and D completes a right-hand orthogonal system (positive eastward). A 19.75-s time offset was discovered in the CCE data after the work by *Takahashi et al.* [1987] was published, and this offset was corrected in Figures 2 and 3. The dashed lines represent the baseline of each component.
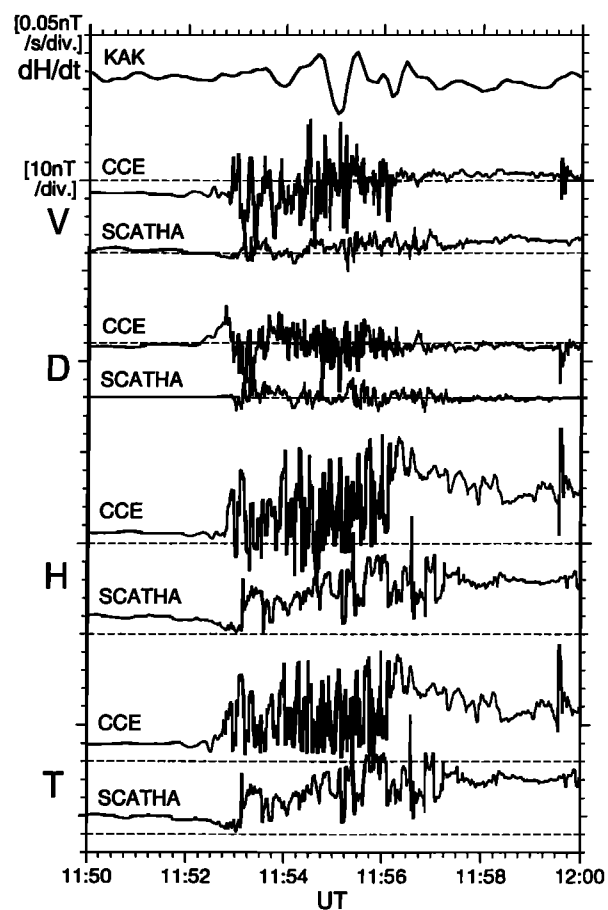

Figure 2. The differentiated H component at the Kakioka ground station (KAK) and the V, D, H, and total field components from the AMPTE/CCE and SCATHA satellites for 1150 to 1200 UT on August 28, 1986.
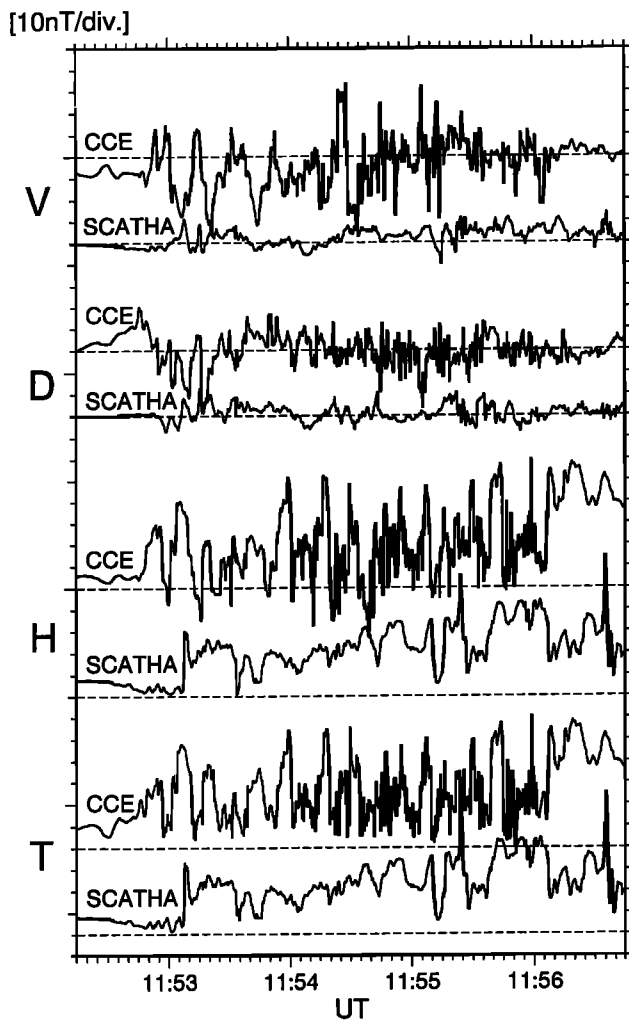
[10nT/div.]

Figure 3. The V, D, H, and total field components from the AMPTE/CCE and SCATHA satellites for 1152:15 to 1156:45 UT on August 28, 1986.

Both AMPTE/CCE and SCATHA observed highly irregular magnetic fluctuations in the middle of the 10-min interval. In the course of the magnetic fluctuations the level of the H component increased substantially at both satellites, indicating that the tail magnetic field changed from a stretched to a more dipolar configuration. The enhancement of the energetic particle flux was also observed at the satellites (not shown; for AMPTE/CCE, see *Takahashi et al.* [1987, Figure 1]). At Kakioka the major perturbation of a Pi2 pulsation started at 1153:30 UT. The irregular magnetic fluctuations at the satellites started simultaneously with, possibly several tens of seconds before, the Pi2 onset; the time delay may be ascribed to communication by an MHD wave between the magnetosphere and the ionosphere. This Pi2 onset was accompanied by an enhancement of the westward electrojet observed at the Cape Wellen ground station (invariant latitude: 62.3°; ~0030 LT), which was located in the same local time sector as the foot point of AMPTE/CCE (although the major enhancement did not occur until 1200 UT) [*Lui et al.*, 1992]. Therefore we infer that the two spacecraft were located in or very close to the onset region and that the observed fluctuations were related to the substorm onset.

Before the commencement of the magnetic fluctuations, at AMPTE/CCE the V component was persistently negative, and its magnitude was very similar to that of the H component, whereas at SCATHA the magnitudes of both V and D components were only a few nanoteslas. It is therefore inferred that AMPTE/CCE was close to, but off, the magnetic equatorial plane, while SCATHA was at the magnetic equator. Since AMPTE/CCE and SCATHA were separated by only a few tenths of a degree in the magnetic latitude, the difference in the magnetic inclination at the two satellite positions suggests that the tail magnetic field was extremely stretched before the magnetic fluctuations started. After the magnetic fluctuations the V component was positive at both AMPTE/CCE and SCATHA, indicating that the location of the neutral sheet shifted upward in the course of the magnetic fluctuations. Despite some similarities of overall features, there are at least four differences between the AMPTE/CCE and SCATHA measurements.

First, AMPTE/CCE observed a large D deviation before the commencement of the magnetic fluctuations, but we cannot find any corresponding signature in the SCATHA data. The peak amplitude of the D deviation at AMPTE/CCE was more than 20 nT, and at that time the magnetic field was almost in the azimuthal direction. Since the V component, which is a good indicator of the spacecraft distance from the magnetic equator, does not show any systematic change that can be associated with the D deviation, we infer that this D deviation was a temporal structure and was localized around AMPTE/CCE. Note also that the H component suddenly started to increase at 1152:45 UT when the D component took its maximum (Figure 3), which was the beginning of the magnetic fluctuations. Thus the deflection of the magnetic field might be related to the excitation of the magnetic fluctuations; however, such a large D deviation is not very common in the other tail current disruption events reported by *Lui et al.* [1992].

Second, when the magnetic fluctuations started at AMPTE/CCE, the H component started to decrease at SCATHA, where the onset of magnetic fluctuations was delayed from the onset at AMPTE/CCE by a few tens of seconds. This H decrease at SCATHA may be interpreted in terms of the further stretching of the tail magnetic field outside of a substorm wedge current system; note that the separation between AMPTE/CCE and SCATHA is mostly in the azimuthal direction (Figure 1).

Third, the amplitude of the fluctuations was significantly larger at AMPTE/CCE than at SCATHA. The H component turned negative many times at AMPTE/CCE, whereas it remained positive at SCATHA. Note also that the V component changed its sign frequently at AMPTE/CCE. These facts indicate that something very dynamic happened at AMPTE/CCE. Considering the second point and the timing relative to the ground Pi2 onset, we infer that AMPTE/CCE was located in the onset region and that SCATHA was slightly away from the onset sector.

Finally, at AMPTE/CCE the characteristics of the magnetic fluctuations changed after 1154 UT, when shorter-timescale fluctuations started (Figure 3). SCATHA did not observe any corresponding fluctuation. At AMPTE/CCE, energetic particle fluxes were enhanced apparently in association with these short-timescale fluctuations, followed by a further enhancement that took place concurrently with the level shift of the H component [*Lui et al.*, 1992, Plate 2].

2.1.2. Magnetic fluctuations. The procedure of the fractal analysis we adopted for this study was developed by *Higuchi*

[1988, 1990]; the basic idea of the method is also described in paper 1. The method consists of two parts. Assume that $X(t)$ is a one-dimensional sequential data set. The first part of the analysis is to calculate the length L of $X(t)$, which is defined as the summation of absolute values of differences between two measurements separated by a timescale τ, then divided by τ: $L(\tau) = \{\Sigma \ |X(t + \tau) - X(t)|\}/\tau$ (see Higuchi [1988, 1990] for the precise expression). Therefore L is a function of τ: $L = L(\tau)$. In the following, L is divided by the interval of an analyzed period so that we can compare L for different periods. The second part is to examine the dependence of $L(\tau)$ on τ. It is known that $L(\tau)$ is often described as a power of τ, that is, $L(\tau) \propto \tau^{-D}$. In such a case the plot $X(t)$ is self-affine, and the power spectrum density of $X(t)$, $P(f)$, is also described as a power of frequency, that is, $P(f) \propto f^{-\alpha}$, where α is related to D as $\alpha = 5 - 2D$. D is referred to as fractal dimension. If $X(t)$ has a characteristic timescale T_c, the doubly logarithmic plot of $L(\tau)$ versus τ has a kink at $\tau = \tau_c$. T_c is 3–5 times τ_c, $T_c = 3 \sim 5\tau_c$ [Higuchi, 1989]. The parameters such as D and τ_c are determined by the least squares fit in this study.

In paper 1 we applied the fractal analysis to the AMPTE/CCE measurements during the interval of 1152:45 to 1154:15 UT, which is after the commencement of the magnetic fluctuations but before the appearance of the higher-frequency variations (Figure 3). We found that the L versus τ plot of the H component has a kink at 4 s. Figure 4a plots $L(\tau)\cdot\tau^{1.3}$, instead of $L(\tau)$, against τ for each magnetic component. The power of τ, 1.3, is the fractal dimension of the H component at $\tau < 4$ s. This is the reason why the plot of the H component is almost flat at $\tau < 4$ s. (Both the kink of the plots and the difference among the components can be seen more clearly in this new format than in the previous format of Figure 5b of paper 1.) $L(\tau)\cdot\tau^{1.3}$, and therefore $L(\tau)$, is largest for the H component except for $\tau > 9$ s. The characteristics of the V and D component variations, such as characteristic timescale, are different from those of the H component variations. In comparison with the H component, the V and D components are sensitive to the distance from the magnetic equator. It is therefore possible that the variations of these components are mixed effects of local waves and satellite motion relative to the spatial structure of these components. For more detailed comparison among the components, see paper 1.

We did the same analysis for the SCATHA measurement. The result is shown in Figure 4b. For SCATHA we selected the interval of 1153:10 to 1154:15 UT; the end time is the same as that for the AMPTE/CCE analysis, but the start time was chosen to be after the commencement of the magnetic fluctuations at the SCATHA location. The amplitude of the H component fluctuations is largest among the three components, as we found for the AMPTE/CCE measurements. At SCATHA the amplitude of the D component variation is larger than that of the V component variation except for a long (>10 s) timescale range, whereas at AMPTE/CCE the order is opposite. The bumps of the V and H component plots around $\tau = 10$ s are likely the result of statistical uncertainty; the duration of the interval analyzed is only several times τ, making it possible to pick up incidental structures. Note also that in Figure 4 the behavior of $L(\tau)$ in the long-timescale range is emphasized by being multiplied by $\tau^{1.3}$.

Since the relative location of each satellite to the neutral sheet changed in the course of the magnetic fluctuations, the observed fluctuations are expected to be partly a spatial effect.
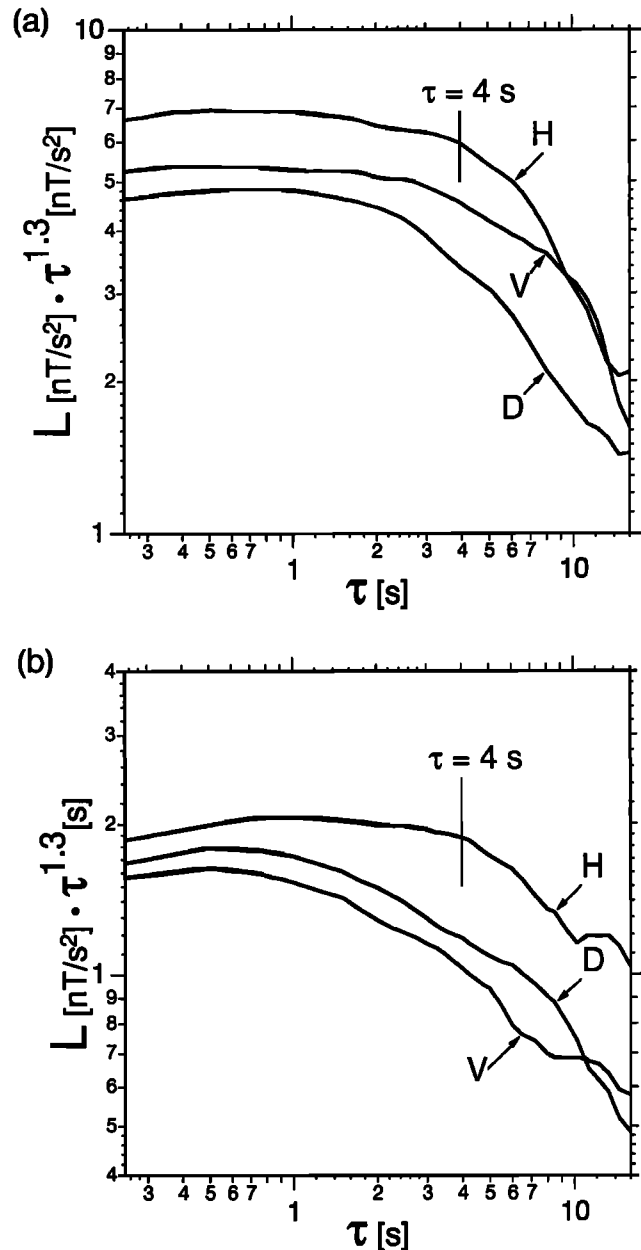

Figure 4. Results of the fractal analysis for the magnetic fluctuations measured by (a) AMPTE/CCE for 1152:45 to 1154:15 UT and (b) SCATHA for 1153:10 to 1154:15 UT. $L(\tau)\cdot\tau^{1.3}$ is plotted against τ for the three magnetic components.

However, the spatial effect should not be the major cause of the fluctuations. In contrast to the V and D components, the H component is insensitive to the distance from the neutral sheet. Thus, if the fluctuations were associated with the motion of the neutral sheet, the amplitude of the V or D component should be largest, which is inconsistent with the observation. Therefore we conclude that the magnetic fluctuations are mostly local waves rather than a spatial effect.

Figure 5 compares the characteristics of the AMPTE/CCE and SCATHA H component fluctuations, where $L(\tau)$ is plotted against τ for both satellites. The solid straight lines, which almost trace the plot of $L(\tau)$, especially at $\tau < 4$ s, present the results of the least squares fit. The amplitude of the magnetic fluctuations, $L(\tau)$, is larger at AMPTE/CCE than at SCATHA
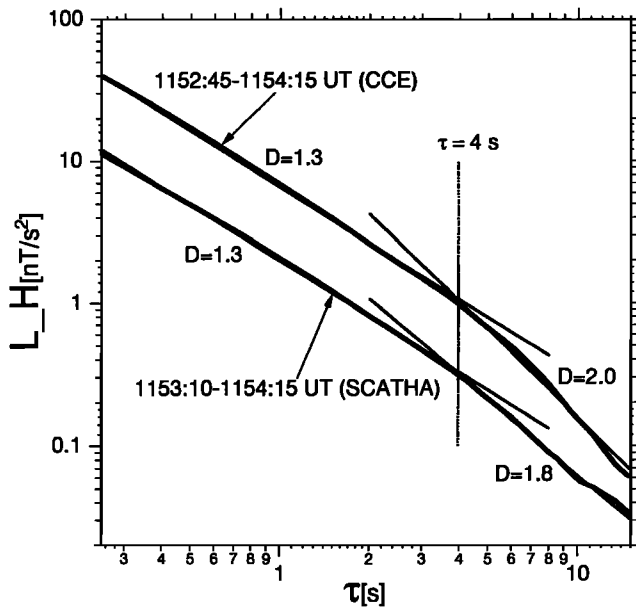
Figure 5. Comparison of the H component magnetic fluctuations observed by AMPTE/CCE and SCATHA on August 28, 1986. $L(\tau)$ is plotted against τ.

by a factor of 3–4, as expected from the visual examination of Figures 2 and 3. The fractal dimension at $\tau > 4$ s is 2.0 for AMPTE/CCE, whereas it is 1.8 for SCATHA, suggesting that in this timescale range the H component variation is more irregular at AMPTE/CCE than at SCATHA.

Except for these differences the characteristics of the fluctuations are very similar at the two satellites. Both plots have a kink at $\tau = 4$ s and a fractal dimension of 1.3 at $\tau < 4$ s, which corresponds to α ($= 5 - 2D$) $= 2.4$ for the power spectrum. The kink at τ (τ_c) $= 4$ s indicates that the fluctuations do have a characteristic timescale, which is inferred to be 12 to 20 s ($T_c = 3 \sim 5\tau_c$). This is consistent with the visual inspection of the H component plots of Figure 3. The total field strength before the onset, say at 1150 UT, was about 10 nT at both satellites, corresponding to a proton gyroperiod of 6.6 s. The average total field strength during the fluctuations was also similar: 23 nT at AMPTE/CCE and 18 nT at SCATHA, corresponding to a proton gyroperiod of 2.7 and 3.6 s, respectively. Thus the characteristic timescale of the magnetic fluctuations is several times the proton gyroperiod. This result suggests that ions play an important role in the excitation of these magnetic fluctuations.

There are two possible interpretations about the similarities of the fluctuations at the two satellites. One is that the fluctuations were propagating and the two satellites observed the signature which had the same origin. The other is that these fluctuations were excited independently by the same mechanism.

To investigate the first possibility, we did the coherence analysis for the AMPTE/CCE and SCATHA measurements [*Bendat and Piersol*, 1971]. The result is shown in Figure 6a. The power spectrum densities of the AMPTE/CCE and SCATHA data are superposed (top), and the coherence is shown (bottom). (For the comparison between the fractal and fast Fourier transform analyses of the AMPTE/CCE data, see Figure 4 of paper 1.) Here we examined two intervals. One is the interval from 1153:10 to 1154:15 UT (solid lines), the same interval we chose for the fractal analysis of the SCATHA data,

and the other is the interval from 1153:00 to 1156:00 UT (dotted lines), almost the entire interval of the magnetic fluctuations. Irrespective of the interval, the coherence is rather low, less than 0.4, in the entire frequency range; in fact, the phase is not shown in Figure 6a because the coherence is too low to determine it reliably. We could not find any significant coherence for the V or D magnetic field components (Figures 6b and 6c), either, for the longer interval. The coherence for the shorter interval is occasionally high (>0.5), at least partly because of statistical uncertainty. We also examined the cross coherence between the two satellite measurements, such as between the AMPTE/CCE V and SCATHA D components, and found the same tendency (not shown); for the shorter interval, significant coherence (about 0.65) was found only between the AMPTE/CCE V and SCATHA H components around 0.2 Hz, but we could not think of any physical reason for this. Most importantly, no evidence of coherence was found in the frequency range corresponding to the characteristic timescale of the magnetic fluctuations, 12–20 s. We therefore conclude that as long as the linear analysis in the frequency domain can tell, the observed magnetic fluctuations cannot be explained in terms of the propagation of the same effect; they are most likely to be excited locally near each satellite.
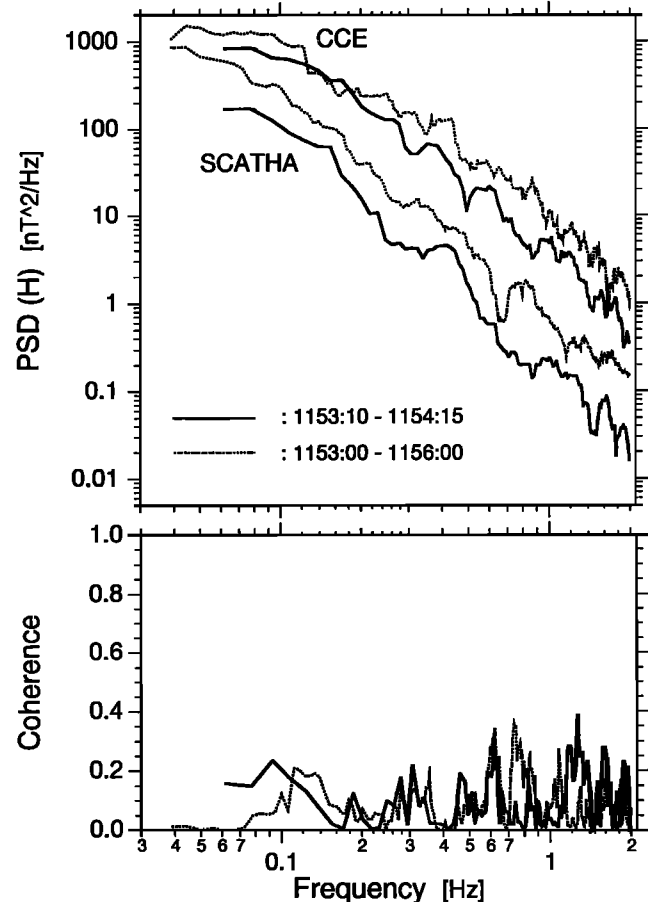

Figure 6a. The coherence between the AMPTE/CCE and SCATHA measurements for the H magnetic component for the intervals of 1153:10 to 1154:15 UT (solid lines) and 1153:00 to 1156:00 UT (dotted lines). (Top) The power spectrum density and (bottom) coherence are plotted. The numbers of the degree of freedom for the spectral estimate, which is twice the N band, are 30 and 18 for the long and short intervals, respectively.
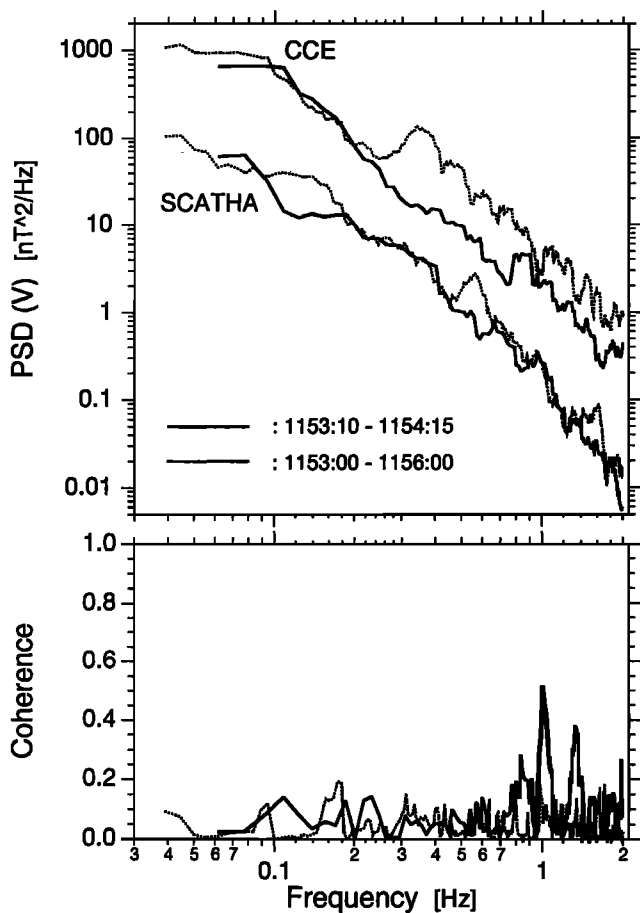
Figure 6b. Same as Figure 6a, except for V magnetic component.

The low coherence between the AMPTE/CCE and SCATHA signatures also indicates that the characteristic spatial scale of the associated electric currents is much shorter than the satellite separation, so that the effects of perturbation currents are canceled out over the satellite separation. The ion Larmor radius (ρ_i) for a perpendicular energy of 6 keV for this event is 1100 km; we assumed that a total magnetic field strength is 10 nT, the value before the onset, whereas the energy is calculated from the preonset ion pressure and density reported by *Lui et al.* [1992] by assuming that all ions are protons. The separation between AMPTE/CCE and SCATHA, 8800 km mostly in the Y direction, corresponds to only $8\rho_i$. Therefore the coherence length of the magnetic fluctuations should be shorter than several proton Larmor radii.

2.2. August 30 (Day 242), 1986, Event

2.2.1. Overall features.
Figure 7 plots the AL index (top) and three magnetic field components of the AMPTE/CCE and SCATHA measurements (bottom) for the August 30 (day 242), 1986, substorm event. The scales of the plots are the same for the two satellites. However, the baselines are different for different components and are indicated on the left and right sides for AMPTE/CCE and SCATHA, respectively. The measurements are presented in GSM coordinates in Figure 7. In this coordinate system the X axis is parallel to the Sun–Earth line, pointing sunward, the Z axis is in the direction of the Earth's

dipole axis projected onto the plane perpendicular to X, and the Y axis completes a right-hand orthogonal system. The dipole tilt angle was 6.2° for this event, and therefore the GSM Z component is practically regarded as the same as the H component: $\cos(6.2°) = 0.994$. The 1-min spin modulation was subtracted from each SCATHA component by applying a Baysian model to wave extraction [*Higuchi,* 1991]; the interval of substorm-associated disturbances was excluded from the determination of the spin modulation. Unfortunately this procedure subtracted low-frequency oscillations with a period similar to the SCATHA spin period, which are clear in the AMPTE/CCE measurement.

Both satellites were located in the premidnight sector just outside of geosynchronous altitude. AMPTE/CCE was outbound, whereas SCATHA was moving mostly dawnward. Two tail reconfiguration (dipolarization) events were observed successively at 0948 and 1004 UT, which are marked by the sharp increases in the Z component; see Figures 8 and 9 for the exact timing. AMPTE/CCE and SCATHA were located at $(-7.0, 2.1, 1.1)$ and $(-7.4, 2.0, 1.0)$ R_E in GSM, respectively, at 0948 UT and at $(-7.2, 1.9, 1.1)$ and $(-7.5, 1.6, 1.0)$ R_E at 1004 UT. The satellite separation was about 0.4 R_E for both events, mostly in the X direction at 0948 UT and equally in the X and Y directions at 1004 UT. SCATHA remained on the tailward side of CCE.

The AL index was at quiet levels (> -100 nT) before 0953 UT, when it started to decrease. *Lui et al.* [1992] examined
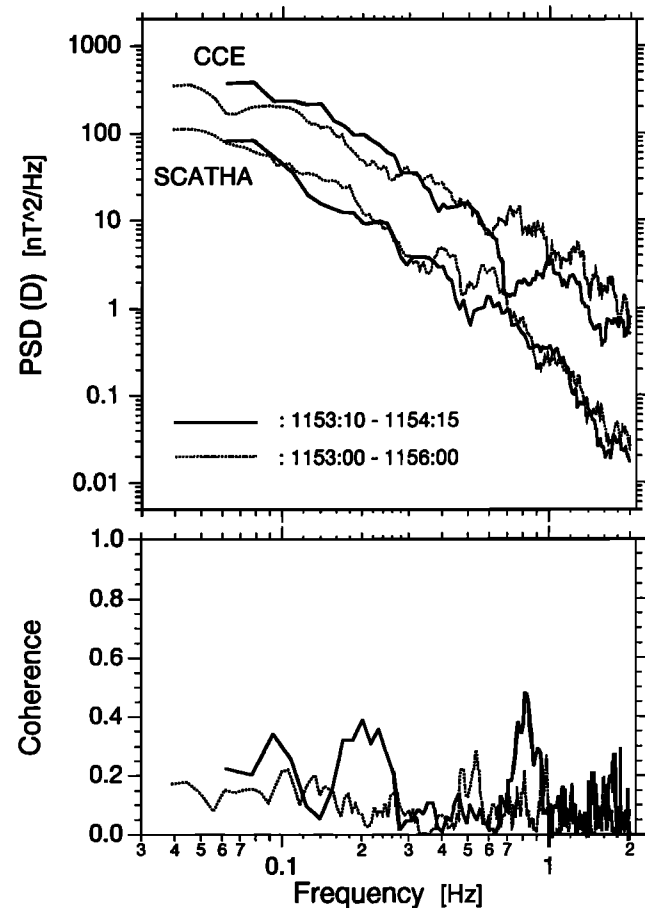

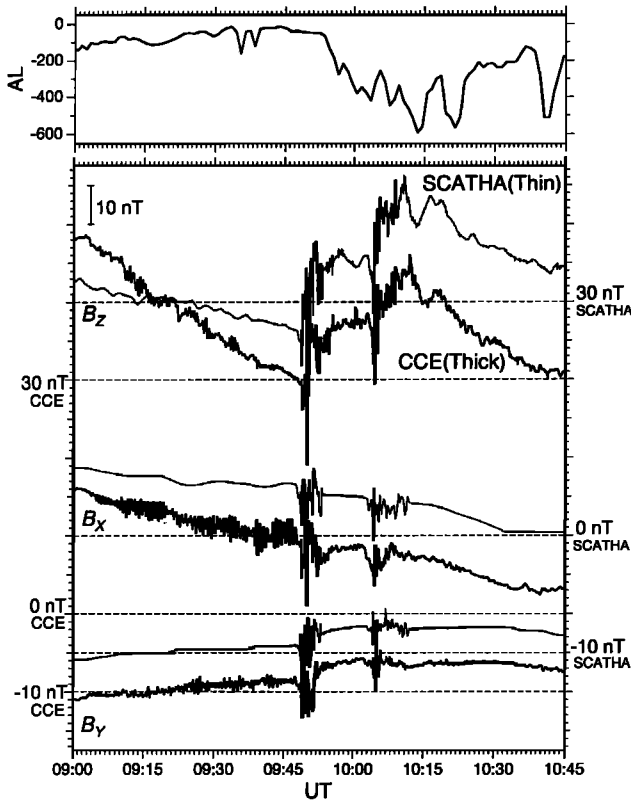**Figure 6c.** Same as Figure 6a, except for D magnetic component.

Figure 7. (Top) The *AL* index and (bottom) 4-s averages of three magnetic field components of the AMPTE/CCE (thick lines) and SCATHA (thin lines) measurements in GSM coordinates for the interval of 0900–1045 UT of August 30, 1986. AMPTE/CCE and SCATHA were located at $(-7.0, 2.1, 1.1)$ and $(-7.4, 2.0, 1.0)$ R_E in GSM, respectively, at 0948 UT and at $(-7.2, 1.9, 1.1)$ and $(-7.5, 1.6, 1.0)$ R_E at 1004 UT, when the Z component increased sharply.

ground substorm signatures for this event. At College (invariant latitude: 64.5°; MLT: 22.5) the Z (vertical) component started to decrease at 0950 UT, suggesting an enhancement of the auroral electrojet intensity poleward of this ground station, and then the H (horizontal) component decreased after a few minutes delay. A ground Pi2 onset was observed at Kakioka at 0949 UT at 19.1 MLT (see Figure 8a). The local time sector of the negative bay subsequently expanded both eastward and westward. Therefore we infer that the satellite measurement of the first B_Z increase was related to a substorm onset; the satellite onset occurring earlier than the ground onset by at least 30 s is similar to what we saw for the August 28, 1986, event and can presumably be ascribed to communication between the magnetosphere and the ionosphere. The second B_Z increase at 1004 UT seems to be related to an intensification of an auroral electrojet; the associated Pi2 onset was observed at 1002 UT at Kakioka.

B_Z tended to decrease before the first B_Z increase, indicating that the tail magnetic field was stretched during the substorm growth phase. The larger magnitude of the B_Z decrease at AMPTE/CCE does not mean that the stretching was localized around that satellite, but it is mostly ascribed to the outward movement of the satellite; AMPTE/CCE was at $X = -6.05$ R_E at 0900 UT. At AMPTE/CCE energetic particle fluxes [*Lui et al.*, 1992, Plate 3] started to increase at 0949 UT. The Z com-

ponent never turned southward at either satellite. In contrast to the August 28, 1986, event, both AMPTE/CCE and SCATHA X components continued to be positive except during several short (less than a few seconds) intervals (see also Figures 8 and 9), indicating that the two satellites stayed off the equatorial plane during most of the interval of the magnetic fluctuations.

2.2.2. Magnetic fluctuations. Figure 8 plots the Kakioka Pi2 data (top) and satellite magnetic field measurements (bottom) for the 4-min interval starting at 0947:30 UT. Major fluctuations associated with a Pi2 onset started around 0949 UT; background fluctuations make it difficult to uniquely determine the timing of the onset. The SCATHA Z component started to
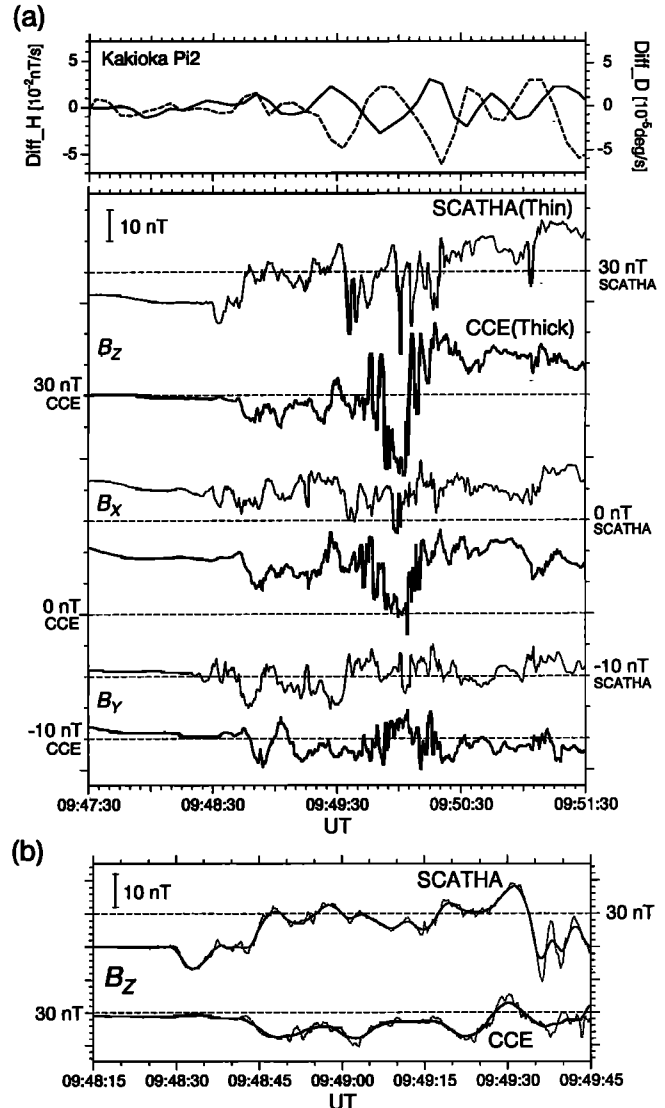

Figure 8. (a) (Top) Differentiated H (solid line) and D (dashed line) magnetic components from the Kakioka ground station and (bottom) AMPTE/CCE and SCATHA magnetic field measurements during the first tail reconfiguration event of the August 30, 1986, substorm. Plotted are three magnetic components in GSM coordinates during the 4-min interval of 0947:30 to 0951:30 UT. (b) The AMPTE/CCE and SCATHA Z components during 0948:15 to 0949:45 UT. The dotted lines represent the observations, and the solid lines represent sliding averages over τ_c, which is 2.8 and 5.1 s for SCATHA and AMPTE/CCE, respectively.

fluctuate irregularly, following the 6-nT dip of the Z component at 0948:30 UT. Fluctuations started several seconds earlier in the X and Y components. Note that these fluctuations started before the Pi2 onset. The AMPTE/CCE Z component also decreased initially, delayed from the SCATHA signature by 15 s, then followed by irregular variations. A similar or even longer delay can be found for the other components. The apparent velocity of the earthward propagation, 180 km/s, which is obtained by dividing the satellite separation by the delay time, is too small to ascribe the time delay to the propagation of the fast magnetosonic mode; note that the perpendicular propagation velocity of the fast magnetosonic mode is larger than the ion thermal velocity, which is 1700 km/s for a thermal energy of 15 keV, which was calculated from the result of Lui et al. [1992] by assuming that all ions are protons. Therefore, as for the August 28, 1986, event, the time delay suggests the spatial expansion of the tail current disruption region. Assuming an equatorial magnetic field strength of 30 nT (the value of B_Z at AMPTE/CCE) and a proton energy of 15 keV, the proton gyroradius is estimated to be 600 km. The satellite separation, 0.4 R_E, is only several times the proton gyroradius. Therefore we infer that the spatial scale of the trigger instability of the tail current disruption is of the order of the proton gyroradius or less.

Although the amplitudes of the fluctuations were similar at the two satellite positions, the characteristics of the fluctuations were different. The difference is most obvious for the interval immediately after the commencement of the fluctuations. The characteristic timescale appears to be shorter at SCATHA than at AMPTE/CCE. This visual examination can be confirmed by the fractal analysis, for which we selected the intervals of 0948:45–0949:30 UT for SCATHA and 0948:50–0949:45 UT for AMPTE/CCE. The τ_c value was found to be 2.8 and 5.1 s for the SCATHA and AMPTE/CCE measurements, respectively. The former corresponds to a characteristic timescale of 8 to 14 s, and the latter corresponds to 15 to 25 s; the proton gyroperiod is 2.2 s for a magnetic field strength of 30 nT. Figure 8b expands on the SCATHA and AMPTE/CCE Z components for the interval of 0948:15 to 0949:45 UT. The dotted lines represent the original measurements, whereas the solid lines represent sliding averages over each value of τ_c. It is clear that the characteristic timescale of the SCATHA Z component is almost half of that of the same component of AMPTE/CCE.

This result is consistent with our previous analysis of the August 28, 1986, event (section 2.1.2) that the observed fluctuations were excited locally near each satellite and that the characteristic spatial scale of the magnetic fluctuations is of the order of the proton gyroradius or shorter. However, the reason for the difference in the characteristic timescale is not very obvious. The Z magnetic component, which provides an approximate magnetic field strength at the equator, was not very different at AMPTE/CCE and SCATHA. B_Z was actually smaller, and therefore the proton gyroperiod was longer, at SCATHA than at AMPTE/CCE before the commencement of the fluctuations, as expected from the SCATHA location farther tailward of AMPTE/CCE. Therefore the longer timescale of the magnetic fluctuations at AMPTE/CCE than at SCATHA indicates that the proton gyration is an important factor but is not the only factor that controls the trigger instability of the tail current disruption.

Figure 9 shows the AMPTE/CCE and SCATHA magnetic field measurements during the 8-min interval (1001–1009 UT) around the second B_Z increase of the August 30, 1986, event.
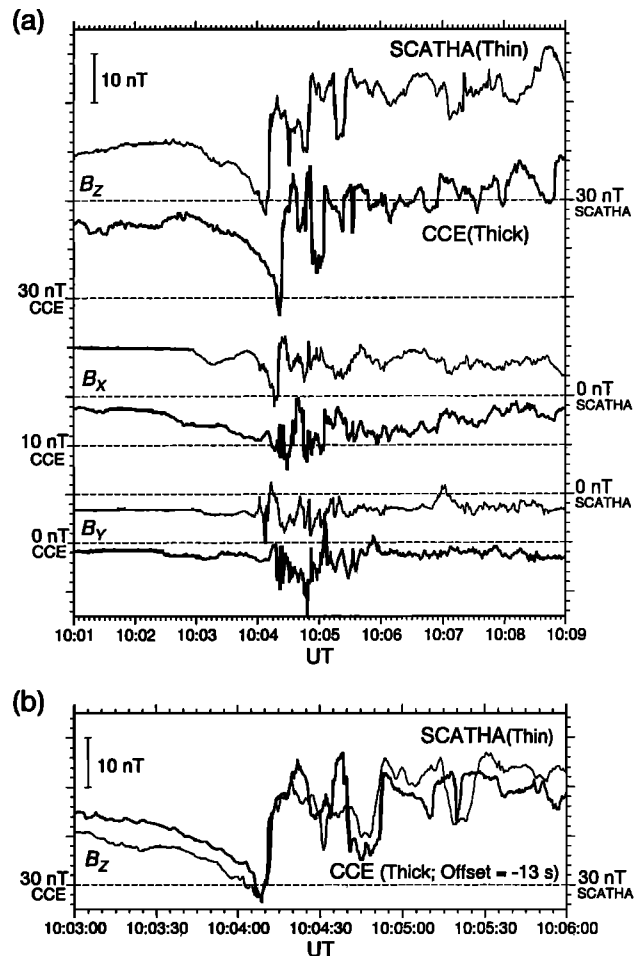

Figure 9. (a) AMPTE/CCE and SCATHA magnetic field measurements for the interval of 1001 to 1009 UT. (b) The AMPTE/CCE (thick line) and SCATHA (thin line) Z components during 1003 to 1006 UT. The time of the AMPTE/CCE measurements is shifted by −13 s.

AMPTE/CCE was located 0.22 R_E earthward and 0.30 R_E duskward of SCATHA. The initial B_Z signature was remarkably similar at the two satellite locations. B_Z decreased by more than 10 nT during the last 1-min interval before the sharp recovery. This B_Z decrease indicates that the tail magnetic field was stretched significantly just before the local onset of the tail magnetic field reconfiguration. In other words, the tail current intensity was enhanced explosively before the local onset of the tail current disruption [Ohtani et al., 1992b]. The onset of the B_Z recovery occurred first at SCATHA and then at AMPTE/CCE with a time lag of 13 s. The fluctuations of the other components also started first at SCATHA. The apparent propagation/expansion velocity, about 200 km/s, is again too slow to explain the observed time lag in terms of the propagation of a fast magnetosonic wave.

For this event the characteristics of the magnetic fluctuations, especially the B_Z fluctuations, look similar at the two satellites. The result of the fractal analysis indicates $\tau_c = 5.0$ s for SCATHA (1004:15–1005:31 UT) and $\tau_c = 5.6$ s for AMPTE/CCE (1004:30–1005:46 UT). Therefore the characteristic timescale of the B_Z fluctuations T_C was 15–25 s and was similar at the two satellite positions.

Figure 9b superposes the AMPTE/CCE (thick line) and SCATHA (thin line) B_Z components during 1003–1006 UT.

The vertical scale is the same for both satellites. The time of the AMPTE/CCE measurements is offset by −13 s so that the commencement of the B_Z recovery matches between the two plots. Although the agreement of the amplitude or timing of each variation is not perfect, some similarities are obvious between the two plots. Thus, for the present event the AMPTE/CCE and SCATHA signatures may be interpreted in terms of the movement of the same current system, which passed by SCATHA and then AMPTE/CCE. This is a remarkable contrast to the August 28, 1986, event, for which we could not find any significant coherence between the two satellite measurements.

Using the apparent propagation/expansion velocity of 200 km/s and the characteristic timescale of the magnetic fluctuations of 20 s, the characteristic spatial scale is estimated to be 4000 km, which is about 7 times the proton gyroradius and is larger than the satellite separation, 0.4 R_E (2500 km); however, this should be regarded as a maximum possible scale because, in general, the satellite separation is not aligned to the direction of the propagation/expansion of the phenomenon. In contrast, the satellite separation was larger for the August 28, 1986, event: 1.4 R_E. Thus the difference between the present event and the August 28, 1986, event may be explained in terms of the intersatellite distance.

2.3. Summary of Observations

Table 1 summarizes the results of the analysis of the August 28 (event 1) and 30 (events 2 and 3), 1986, events; from now on we refer to each event according to its sequential number. Listed are the date and universal time of the events, the satellite positions in GSM, the satellite separation vector ($r_S − r_C$) pointing from AMPTE/CCE (r_C) to SCATHA (r_S), the separation distance ($|r_S − r_C|$); the sequence of dipolarization ($C \rightarrow S$: a local onset took place first at AMPTE/CCE and then at SCATHA, and vice versa), the proton gyroradius corresponding to the average perpendicular energy calculated from *Lui et al.* [1992] (6 keV for event 1 and 15 keV for events 2 and 3), the characteristic timescale of the magnetic fluctuations (τ_c and T_c) at each satellite, the proton gyroperiod, and the coherence between the two satellite measurements. For the calcu-

lation of the proton gyroradius and gyroperiod we used the north–south magnetic field component at AMPTE/CCE before the commencement of the fluctuations, 10 nT for event 1 and 30 nT for events 2 and 3. For the gyroperiod, Table 1 also lists the values calculated from the average magnetic field strength during the fluctuation.

3. Discussion

In section 2 we examined substorm-associated magnetic variations observed by the AMPTE/CCE and SCATHA spacecraft on August 28 and 30, 1986. In these events the local magnetic field changed from a stressed to a more dipolar configuration in the course of the magnetic fluctuations, suggesting that the magnetic fluctuations are associated with tail current disruption. In the following we will discuss the timescale and spatial scale of the fluctuations and will address what constraint the result of the present study can place on modeling studies of the substorm trigger.

This study, as well as paper 1, revealed that the magnetic fluctuations do have a characteristic timescale, which is a few to several times the proton gyroperiod. One may attempt to interpret the magnetic fluctuations in terms of ion cyclotron waves. However, this idea is not supported because the linear kinetic theory indicates that the ion cyclotron instability has maximum growth at parallel propagation, for which an excited wave is not compressional [e.g., *Gary*, 1992]. This is not consistent with the significant variations of the total field strength observed during the event (Figures 2 and 3).

Although the present result suggests that ions play an important role in the generation of the magnetic fluctuations, what determines the characteristic timescale is still to be understood. In events 1 and 3 the timescales were practically the same at AMPTE/CCE and SCATHA. In contrast, in event 2 the difference in the timescale at the two satellite positions was significant (Figure 8b) despite the small satellite separation, 0.4 R_E; τ_c was 2.8 s and 5.1 s at SCATHA and AMPTE/CCE, respectively. We also note that the background field strength was weaker and therefore the gyroperiod was longer in event 1 than in event 3, whereas τ_c was smaller in event 1. These results in-

Table 1. Summary of the Analysis of the August 28 (Event 1) and August 30 (Events 2 and 3), 1986, Events

	Event 1	Event 2	Event 3
Universal Time	1153	0948	1004
Position (GSM, R_E)			
CCE (r_c)	(−7.8, 1.2, 1.5)	(−7.0, 2.1, 1.1)	(−7.2, 1.9, 1.1)
SCATHA (r_s)	(−7.5, −0.1, 1.3)	(−7.4, 2.0, 1.0)	(−7.5, 1.6, 1.0)
Separation			
($r_s − r_c$), R_E	(0.3, −1.3, −0.2)	(−0.4, −0.1, −0.1)	(−0.2, −0.3, −0.1)
$|r_s − r_c|$, R_E/km	1.4/8800	0.4/2700	0.4/2500
Sequence	$C \rightarrow S$	$S \rightarrow C$	$S \rightarrow C$
Proton gyroradius, km	1100	600	600
$\tau_c(T_c)$, s			
CCE	4.0 (12–20)	5.1 (15–25)	5.6 (17–28)
SCATHA	4.0 (12–20)	2.8 (8–14)	5.0 (15–25)
Proton gyroperiod (preonset/average B), s	6.6/2.7	2.2/2.0	2.2/1.3
Coherence	no	no	yes

dicate that there are other factors that determine the timescale of the fluctuations; such factors might be related to the spatial scale of the fluctuations or to the velocity of particles.

Holter et al. [1995] also recently examined the characteristic timescale of substorm-associated magnetic fluctuations. They applied the wavelet transform to magnetic field and electric field fluctuations observed at a substorm breakup by the GEOS geosynchronous satellite; the event was previously reported by *Roux et al.* [1991]. They found that oscillations with periods of 45 to 65 s developed prior to the onset. This timescale is a few times, though of the same order as, the result of this study and paper 1. However, the excitation mechanism is perhaps different. This is so because at the GEOS 2 position the magnetic field was as strong as 60 nT, and therefore the determined timescale was several tens of times the local proton gyroperiod. *Holter et al.* [1995] interpreted the oscillations as wave modes trapped in a current layer. The difference of the timescale may suggest different trigger mechanisms. *Roux et al.* [1991] and *Holter et al.* [1995] discussed this event in detail in terms of the ballooning instability; however, the ballooning stability of the preonset near-Earth magnetotail is debatable [*Ohtani and Tamao*, 1993].

The comparison between the AMPTE/CCE and SCATHA measurements indicates that the spatial scale of the magnetic fluctuations is of the order of the proton gyroradius or could be even shorter. The observed time lag between the onsets of magnetic variations at the two satellites cannot be explained in terms of wave propagation. Furthermore, in event 1 the coherence of the magnetic fluctuations at AMPTE/CCE and SCATHA was rather low (Figure 6) despite the similar characteristics of the fluctuations and the small satellite separation, 1.4 R_E (8 times the proton gyroradius). In event 2 even the characteristic timescale was different at the two satellites, which were separated by 0.4 R_E (several times the proton gyroradius). These results strongly suggest that the magnetic fluctuations were excited locally.

In contrast, for event 3 the B_Z signatures observed by AMPTE/CCE and SCATHA reveal some similarities. However, even for this event, the apparent propagation speed, 200 km/s, is too small to ascribe the observed time lag to the propagation of a fast magnetosonic wave. Instead, the similarity of the B_Z signatures may be explained in terms of the earthward plasma convection, which conveys the associated perturbation currents and therefore the magnetic fluctuations with plasma. SCATHA was located tailward of AMPTE/CCE. Therefore the sense of the observed time delay, that is, first at SCATHA and then at AMPTE/CCE, is consistent with this idea. A convection velocity of 200 km/s and a total field strength of 30 nT require an electric field of 6 mV/m, which is not uncommon during a substorm [*Aggson et al.*, 1983]. The earthward expansion of the tail current disruption region is examined in a separate paper [S. Ohtani, Earthward expansion of tail current disruption: Dual-satellite study, submitted to *Journal of Geophysical Research*, 1997].

In event 1 the amplitude of the H component fluctuation is larger than, but does not overwhelm, the amplitudes of the fluctuations of the other components (Figure 4); this was also confirmed for events 2 and 3 as well as for other AMPTE/CCE events (paper 1). Thus we infer that electric currents associated with these fluctuations flow in various directions but flow preferentially perpendicular to the H axis, that is, parallel to the tail current sheet. Since the peak-to-peak amplitude of the H com-

ponent variation at AMPTE/CCE is several tens of nanoteslas, which is comparable to the net H increase associated with the tail reconfiguration (dipolarization), the local variation of the cross-tail current must be substantial. Considering that a substorm onset is generally characterized by an increase in the H component farther earthward at geosynchronous altitude [e.g., *Kokubun and McPherron*, 1981], we infer that these perturbation currents are actually related to changes in the cross-tail current intensity.

From these results we suggest that the tail current disruption is described as a system of filamentary electric currents, which flow in various directions but flow preferentially antiparallel to the cross-tail current. This idea is schematically depicted in Figure 10, in which the spatial scale is denoted on the basis of the AMPTE/CCE and SCATHA observations of event 1 (the basic concept of the figure was adopted from *Lui et al.* [1988, Figure 4]). The comparison between the AMPTE/CCE and SCATHA measurements suggests that even inside the current disruption region the effects of filamentary currents are averaged out within several proton Larmor radii. Farther away from the disruption region only the net effect of such a random current system can be detected, and the resultant magnetic signature, dipolarization, can be explained in terms of a decrease in the tail current intensity.

The results of this study place several important constraints on modeling studies of the substorm trigger (see *Lui* [1991], *Fairfield* [1992], and articles in the special section "Magnetospheric Substorms: Invited Reviews" in *Joural of Geophysical Research* (*101*(A6), 12,937–13,113, 1996) for recent reviews). First, we found that both temporal and spatial scales of tail current disruption signatures are probably outside of, though could be at the marginal edge of, the ranges of the MHD approximation. Therefore, even though the global dynamics of near-Earth substorm process may be simulated in the MHD framework [*Hesse and Birn*, 1991; *Birn and Hesse*, 1996], the kinetic treatment is essential for describing the tail current disruption, at least for the events examined in this study.

Second, because the timescale of the fluctuations is much shorter than the communication time (Alfvén transit time) between the magnetosphere and the ionosphere, which is inferred to be of the same order as that of Pi2 pulsations, 40 to 150 s, this study suggests that the trigger of a substorm is determined
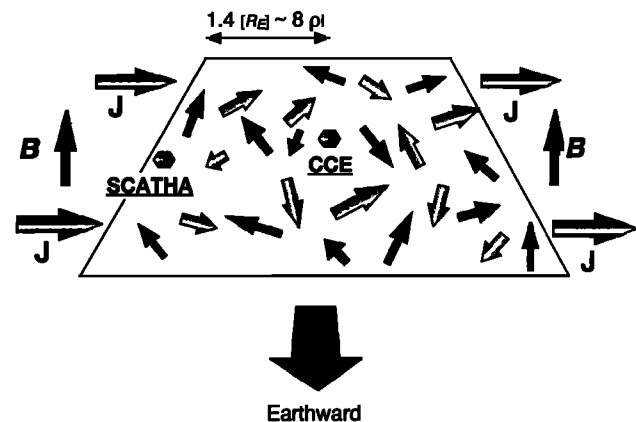

Figure 10. A schematic diagram of the tail current disruption illustrating the chaotic features of magnetic field and electric current perturbations in the onset region. The basic concept was adopted from *Lui et al.* [1988, Figure 4].

by a local condition in the magnetosphere. However, we emphasize that this fact does not lessen the importance of the ionosphere for the substorm processes. It is perhaps true that the local condition is determined by more global processes in which the ionosphere plays an important role. We also note that the intensity of a substorm following the onset is likely to depend on ionospheric conditions such as conductivities [e.g., *Kan et al.*, 1988].

There are two substorm trigger models in which the kinetics of ions play an essential role. One of them, to which theorists have paid more attention than any other substorm model, is the tearing mode instability. *Schindler* [1974] proposed that ions are unmagnetized near the neutral sheet because their Larmor radius is comparable to the field line curvature radius, and such ions destabilize the (ion) tearing mode. It is suggested that the instability strongly depends on the behavior of electrons, such as pitch angle scattering by waves [*Coroniti*, 1980; *Kuznetsova and Zelenyi*, 1991] and nonadiabatic stochastic diffusion [*Büchner and Zelenyi*, 1989]. However, some recent studies [*Pellat et al.*, 1991; *Brittnacher et al.*, 1994] claim that these effects are not efficient enough to remove the strong stabilization caused by electron compressibility. The question of the ion tearing mode instability remains controversial.

The other kinetic model of the substorm trigger is the cross-field streaming instability. *Lui et al.* [1991] applied this instability to the neutral sheet environment. Also, in this instability, unmagnetized ions play an important role. The real frequency of unstable modes was determined to be in a range of 0.02 to 2 Hz, corresponding to a period of 0.6 to 60 s, based on parameters obtained from observations. The model also predicts that the wavelength of unstable modes is 0.7 to 3.6 times the proton gyroradius (the values are calculated from *Lui et al.* [1991, Figures 4 and 6] for an ion-to-electron temperature ratio of 4). The characteristic timescale and the coherence length of the magnetic fluctuations, which we determined in this analysis, are in the ranges expected for this instability.

In closing, we note that this study was motivated by the AMPTE/CCE observations of the magnetic fluctuations associated with the substorm trigger. Such magnetic fluctuations may be associated with every substorm onset but can be observed only occasionally because of the limited spatial coverage of the satellite observation. However, it is also possible that the magnetic fluctuations represent only one class of substorms and that there are different classes of substorms that are triggered by different instabilities, including MHD instabilities such as the ballooning instability. We need to be cautious when applying the result of this study to other substorm events.

4. Summary

In this study we examined magnetic fluctuations observed by the AMPTE/CCE and SCATHA satellites in the near-Earth magnetotail during the August 28 and 30, 1986, substorm events. We confirmed the finding of our previous study (paper 1). That is, (1) the magnetic fluctuations do have a characteristic timescale, which we found to be a few to several times the proton gyroperiod, and (2) the amplitude of the H (Z) component fluctuation is larger than but does not overwhelm the amplitudes of the fluctuations of the other components. The first point suggests that ions play an important role in the excitation of the magnetic fluctuations, and the second point indicates that

associated electric currents flow preferentially parallel to the equatorial plane.

The comparison between the AMPTE/CCE and SCATHA observations allowed us to address the spatial scale and development of the magnetic fluctuations. Despite the small satellite separation, which is less than 10 times the proton gyroradius, the coherence between the AMPTE/CCE and SCATHA measurements was found to be low for the August 28, 1986, event (event 1). In the first event of August 30, 1986 (event 2), even the characteristic timescale was different at the two satellite locations, whereas some similarities were found between the AMPTE/CCE and SCATHA B_Z signatures for the second event of August 30, 1986 (event 3), which may be interpreted in terms of earthward plasma convection. We also found that the two satellites observed a noticeable time delay of the commencement of the magnetic fluctuations. The apparent propagation velocity was significantly smaller than the phase velocity of the fast magnetosonic mode. Therefore the observed magnetic fluctuations cannot be regarded as a remote effect of a change in the current intensity that took place away from the satellites. These results strongly suggest that the magnetic fluctuations are excited locally and that the characteristic scale of the fluctuations is of the order of the proton gyroradius or even shorter. We infer that the tail current disruption is described as a system of filamentary currents that flow in various directions but flow preferentially antiparallel to the tail current. Effects of such perturbation currents are canceled out away from the current disruption region so that the resultant magnetic signature, which is often called dipolarization, is well described in terms of the reduction of the tail current intensity. Although this study does not identify the trigger mechanism of the tail current disruption, we infer that the tail current disruption is a local and kinetic process in which ions play an important role.

References

Aggson, T. L., J. P. Heppner, and N. C. Maynard, Observations of large magnetospheric electric fields during the onset phase of a substorm, *J. Geophys. Res.*, *88*, 3981, 1983.

Bendat, J. S., and A. G. Piersol, *Random Data: Analysis and Measurement Procedures*, p. 407, John Wiley, New York, 1971.

Birn, J., and M. Hesse, Details of current disruption and diversion in simulations of magnetotail dynamics, *J. Geophys. Res.*, *101*, 15,345, 1996.

Brittnacher, M., K. B. Quest, and H. Karimabadi, On the energy principle and ion tearing in the magnetotail, *Geophys. Res. Lett.*, *21*, 1591, 1994

Büchner, J., and L. M. Zelenyi, Regular and chaotic charged particle motion in magnetotaillike field reversals, 1, Basic theory of trapped motion, *J. Geophys. Res.*, *94*, 11,821, 1989.

Burkhart, G. R., P. B. Dusenbery, T. W. Speiser, and R. E. Lopez, Hybrid simulations of thin current sheets, *J. Geophys. Res.*, *98*, 21,373, 1993.

Coroniti, F. V., On the tearing mode in quasi-neutral sheets, *J. Geophys. Res.*, *85*, 6719, 1980

Elphinstone, R. D., D. Hearn, J. S. Murphree, and L. L. Cogger, Mapping using the Tsyganenko long magnetospheric model and its relationship to Viking auroral images, *J. Geophys. Res.*, *96*, 1467, 1991.

Fairfield, D. H., Advances in magnetospheric storm and substorm research: 1989-1991, *J. Geophys. Res.*, *97*, 10,865, 1992.

Fennell, J. F., Description of P78-2 (SCATHA) satellite and experiments, *The IMS Source Book: Guide to the International Magnetosphere Study Data Analysis*, edited by C. T. Russell and D. J. Southwood, AGU, Washington, D. C., pp. 65-81, 1982.

Gary, S. P., The mirror and ion cyclotron anisotropy instabilities, *J. Geophys. Res.*, *97*, 8519, 1992.

Hesse, M., and J. Birn, On dipolarization and its relation to the substorm current wedge, *J. Geophys. Res.*, *96*, 19,417, 1991.

Higuchi, T., Approach to an irregular time series on the basis of the fractal theory, *Physica D*, *31*, 277, 1988.

Higuchi, T., Fractal analysis of time series (in Japanese), *Proc. Inst. Stat. Math.*, *37*, 209, 1989.

Higuchi, T., Relationship between the fractal dimension and the power law index for a time series: A numerical investigation, *Physica D*, *46*, 254, 1990.

Higuchi, T., Method to subtract an effect of the geocorona EUV radiation from the Low Energy Particle (LEP) data by the Akebono (EXOS-D) satellite, *J. Geomagn. Geoelectr.*, *43*, 957, 1991.

Holter, Ø., C. Altman, A. Roux, S. Perraut, A. Pedersen, H. Pécseli, B. Lybekk, J. Trulsen, A. Korth, and G. Kremser, Characterization of low frequency oscillations at substorm breakup, *J. Geophys. Res.*, *100*, 19,109, 1995.

Jacquey, C., J. A. Sauvaud, and J. Dandouras, Location and propagation of the magnetotail current disruption during substorm expansion: Analysis and simulation of an ISEE multi-onset event, *Geophys. Res. Lett.*, *18*, 389, 1991.

Jacquey, C., J. A. Sauvaud, J. Dandouras, and A. Korth, Tailward propagating cross-tail current disruption and dynamics of near-Earth tail: Multi-point measurement analysis, *Geophys. Res. Lett.*, *20*, 983, 1993.

Kan, J. R., L. Zhu, and S.-I. Akasofu, A theory of substorms: Onset and subsidence, *J. Geophys. Res.*, *93*, 5624, 1988.

Kaufmann, R. L., Substorm currents: Growth phase and onset, *J. Geophys. Res.*, *92*, 7471, 1987.

Kennel, C., The Kiruna conjecture: The strong version, in *Proceedings of the International Conference on Substorms (ICS-1)*, *Eur. Space Agency Spec. Publ., ESA SP-335*, p. 599, 1992.

Kokubun, S., and R. L. McPherron, Substorm signatures at synchronous altitude, *J. Geophys. Res.*, *86*, 11,265, 1981.

Kuznetsova, M. M., and L. M. Zelenyi, Magnetic reconnection in collisionless field reversals: The universality of the ion tearing mode, *Geophys. Res. Lett.*, *18*, 1825, 1991.

Lopez, R. E., and A. T. Y. Lui, A multisatellite case study of the expansion of a substorm current wedge in the near-Earth magnetotail, *J. Geophys. Res.*, *95*, 8009, 1990.

Lopez, R. E., A. T. Y. Lui, D. G. Sibeck, K. Takahashi, R. W. McEntire, L. J. Zanetti, and S. M. Krimigis, On the relationship between the energetic particle flux morphology and the change in the magnetic field magnitude during substorms, *J. Geophys. Res.*, *94*, 17,105, 1989.

Lopez, R. E., H. Lühr, B. J. Anderson, P. T. Newell, and R. W. McEntire, Multipoint observations of a small substorm, *J. Geophys. Res.*, *95*, 18,897, 1990.

Lopez, R. E., H. E. Spence, and C.-I. Meng, DMSP F7 observations of a substorm field-aligned current, *J. Geophys. Res.*, *96*, 19,409, 1991.

Lui, A. T. Y., A synthesis of magnetospheric substorm models, *J. Geophys. Res.*, *96*, 1849, 1991.

Lui, A. T. Y., R. E. Lopez, S. M. Krimigis, R. W. McEntire, L. J. Zanetti, and T. A. Potemra, A case study of magnetotail current sheet disruption and diversion, *Geophys. Res. Lett.*, *15*, 721, 1988.

Lui, A. T. Y., C.-L. Chang, A. Mankofsky, H.-K. Wong, and D. Winske, A cross-field current instability for substorm expansions, *J. Geophys. Res.*, *96*, 11,389, 1991.

Lui, A. T. Y., R. E. Lopez, B. J. Anderson, K. Takahashi, L. J. Zanetti, R. W. McEntire, T. A. Potemra, D. M. Klumpar, E. M. Greene, and R. Strangeway, Current disruptions in the near-Earth neutral sheet region, *J. Geophys. Res.*, *97*, 1461, 1992.

Ohtani, S., and T. Tamao, Does the ballooning instability trigger substorms in the magnetotail?, *J. Geophys. Res*, *98*, 19,369, 1993.

Ohtani, S., K. Takahashi, L. J. Zanetti, T. A. Potemra, R. W. McEntire, and T. Iijima, Tail current disruption in the geosynchronous region, in *Magnetospheric Substorms, Geophys. Monogr. Ser.*, vol 64, edited by J. R. Kan, T. A. Potemra, S. Kokubun, and T. Iijima, p. 131, AGU, Washington, D. C., 1991.

Ohtani, S., S. Kokubun, and C. T. Russell, Radial expansion of the tail current disruption during substorms: A new approach to the substorm onset region, *J. Geophys. Res.*, *97*, 3129, 1992a.

Ohtani, S., K. Takahashi, L. J. Zanetti, T. A. Potemra, R. W. McEntire, and T. Iijima, Initial signatures of magnetic field and energetic particle fluxes at tail reconfiguration: Explosive growth phase, *J. Geophys. Res.*, *97*, 19,311, 1992b.

Ohtani, S., et al., A multisatellite study of a pseudo-substorm onset in the near-Earth magnetotail, *J. Geophys. Res.*, *98*, 19,355, 1993.

Ohtani, S., T. Higuchi, A. T. Y. Lui, and K. Takahashi, Magnetic fluctuations associated with tail current disruption: Fractal analysis, *J. Geophys. Res.*, *100*, 19,135, 1995.

Pellat, R., F. V. Coronitti, and P. L. Pritchett, Does ion tearing exist?, *Geophys. Res. Lett.*, *18*, 143, 1991.

Potemra, T. A., L. J. Zanetti, and M. H. Acuna, The AMPTE/CCE magnetic field experiment, *IEEE Trans. Geosci. Remote Sens.*, *GE-23*(3), 246-249, 1985.

Pulkkinen, T. I., D. N. Baker, D. H. Fairfield, R. J. Pellinen, J. S. Murphree, R. D. Elphinstone, R. L. McPherron, J. F. Fennell, R. E. Lopez, and T. Nagai, Modeling the growth phase of a substorm using the Tsyganenko model and multi-spacecraft observations: CDAW-9, *Geophys. Res. Lett.*, *18*, 1963, 1991.

Roux, A., S. Perraut, P. Robert, A. Morane, A. Pedersen, A. Korth, G. Kremser, B. Aparicio, D. Rodgers, and R. Pellinen, Plasma sheet instability to the westward traveling surge, *J. Geophys. Res.*, *96*, 17,697, 1991.

Samson, J. C., L. R. Lyons, P. T. Newell, F. Creutzberg, and B. Xu, Proton aurora and substorm intensifications, *Geophys. Res. Lett.*, *19*, 2167, 1992.

Schindler, K., A theory of the substorm mechanism, *J. Geophys. Res.*, *79*, 2803, 1974.

Takahashi, K., L. J. Zanetti, R. E. Lopez, R. W. McEntire, T. A. Potemra, and K. Yumoto, Disruption of the magnetotail current sheet observed by AMPTE CCE, *Geophys. Res. Lett.*, *14*, 1019, 1987.

J. F. Fennell, Aerospace Corporation, P.O. Box 92957, M2 259, Los Angeles, CA 90009. (e-mail: joe_fennell@qmail.aero.org)

T. Higuchi, Institute of Statistical Mathematics, Tokyo 106, Japan. (e-mail: higuchi@sunstar.ism.ac.jp)

A. T. Y. Lui and S. Ohtani, Applied Physic Laboratory, Johns Hopkins University, Johns Hopkins Road, Laurel, MD 20723-6099. (e-mail: lui@jhuapl.edu; ohtani@jhuapl.edu)

H. E. Spence, Center for Space Physics, Boston University, 725 Commonwealth Avenue, Boston, MA 02215. (e-mail: spence@bu.edu)

K. Takahashi, Solar-Terrestrial Environment Laboratory, Nagoya University, Toyokawa 442, Japan. (e-mail: kazue@stelab.nagoya-u.ac.jp)